

# Implementing soil radon detectors for long term continuous monitoring

Gianfranco Galli<sup>a\*</sup>, Valentina Cannelli<sup>a</sup>, Adriano Nardi<sup>a</sup>, Antonio Piersanti<sup>a</sup>

<sup>a</sup>Istituto Nazionale di Geofisica e Vulcanologia, Via di Vigna Murata 605, I-00143 Rome, Italy

\*Corresponding author: [gianfranco.galli@ingv.it](mailto:gianfranco.galli@ingv.it) (Gianfranco Galli)

## Abstract

The employment of different instruments for radon continuous measurements within the Italian Radon mOnitoring Network (IRON), mostly INGV, Algade AER and Airthings Corentium instruments, requires a uniform characterization and calibration protocol for the results to be comparable in a rigorous way. A 56 L stainless steel radon chamber with a sensitivity of  $0.95 \pm 0.01$  Bq m<sup>-3</sup> per pulse h<sup>-1</sup> has been used and validation of Algade AER, Airthings Corentium and Durrige RAD7 radon monitors equipped with solid-state detectors operated at different absolute humidity values has been performed, extending their operative range. Robustness to atmospheric electromagnetic phenomena of INGV and Algade AER instruments has been investigated and, for the former instrument, improved.

## Keywords

Soil radon; long term continuous monitoring; lucas cell vs solid-state detectors; calibration; electrical shielding

## 1. Introduction

Radon detectors are employed in a wide range of applications, from environmental safety and public health to Earth sciences studies, especially in the frame of volcanic surveillance and seismic monitoring. The Istituto Nazionale di Geofisica e Vulcanologia in Italy (INGV) hosts the Radionuclide Laboratory where radon instrumentation devoted to all the above applications is managed, set up and developed. In the last years, INGV implemented the Italian Radon mOnitoring Network (IRON), a new nationwide permanent network for near real-time measurements of soil

61  
62  
63 radon emissions in Italy (Cannelli, 2017; Cannelli et al., 2018). Presently IRON consists of 36  
64 stations covering the whole Italian peninsula and represents one of the few examples worldwide of  
65 such a network (in terms of covered area, time series length and total number of stations).  
66

67  
68 The employment of different instruments within a same network, used for discrete or continuous  
69 radon measurements, requires a unified calibration protocol and the certification of their robustness  
70 to variable environmental conditions, so that results are comparable in a rigorous way.  
71

72  
73 Therefore, the manuscript is aimed at *i*) the fulfilment of the above stated requirements, also testing  
74 and improving, if necessary, the instrument electrical shielding and *ii*) the validation of the  
75 behaviour of radon monitors equipped with solid-state detectors operated at high absolute humidity  
76 values, thus extending their operative range and employing possibilities. A radon chamber available  
77 at the INGV Radionuclide Laboratory has been used, calibrated by intercomparison as described in  
78 De Simone et al., 2016.  
79

80  
81 As a matter of fact, monitors equipped with a scintillation cell are not influenced by absolute  
82 humidity, consequently only their calibration and linearity have been assessed. Differently, the  
83 response of radon monitors employing semiconductor detectors needs to be corrected as a function  
84 of absolute humidity (Chu and Hopke, 1988; Hopke, 1989; Roca et al., 2004; Tuccimei et al., 2006;  
85 De Simone et al., 2016), especially if electrostatic collection of the short-lived radon daughters  
86 takes place and/or big sized detection volumes are adopted. Water molecules cause the  
87 neutralization of radon progenies, reducing the detector efficiency (wall attachment, thin water film  
88 onto the detector and, for electrostatic chambers, reduced collection).  
89

90  
91 Corrections can vary for every instrument also because their temperature, humidity and pressure  
92 sensors (when available) are used, consequently also their conditions may affect the monitor  
93 characterization.  
94

## 95 96 97 98 99 100 101 102 103 **2. Materials and methods**

104  
105  
106 A list of radon monitors available at INGV laboratories and/or employed at remote sites follows.  
107

### 108 109 110 **2.1 INGV proprietary instrument**

111 Most IRON stations adopt a high sensitivity proprietary instrument employing an alpha scintillation  
112 detector (a Lucas Cell), consisting of a flask, whose inner wall is coated with silver-activated zinc  
113 sulphide (ZnS). It integrates a front-end electronics for pulse shaping. Radon enters the detector by  
114  
115

121  
122  
123 diffusion through an inlet filter that traps radon daughters. For 500 mL scintillating flasks  
124 (Algade<sup>®</sup>), sensitivity is typically in the range 0.24-0.28 Bq m<sup>-3</sup> per pulse h<sup>-1</sup>, while minimum  
125 detectable concentration is 3-6 Bq m<sup>-3</sup>. The instrument is powered by a 12V lead-acid battery,  
126 which is charged by a power supply connected to 220V mains or to a solar panel, depending on  
127 installation types. Radon measurements are performed by counting the radon decay signals within  
128 an adjustable acquisition time; in old models they are stored locally in the front-end electronics  
129 memory and can be downloaded through a serial interface. In recent models a new acquisition  
130 system with remote transmission based on the open-source Arduino platform  
131 (<https://www.arduino.cc/>) has been implemented; this low-cost, low-power data acquisition device  
132 can provide both local storage on a flash memory and real-time data transmission via the Global  
133 System for Mobile Communications (GSM) network (Cannelli et al., 2018).  
134  
135  
136  
137  
138  
139  
140  
141

## 142 **2.2 Algade AER**

143  
144 Algade AER Plus (<http://www.algade.com/>) is a small sized commercial solid-state radon detector,  
145 providing also local storage for temperature and relative humidity data. The connected version  
146 (AER C) is available for data transmission by Internet of Things (IoT) Sigfox protocol  
147 (<https://www.sigfox.com/en>), where data are retrieved connecting with a client to an Algade server.  
148 Instruments are battery supplied with autonomy of one year. Since 2017, we started to test and  
149 deploy AER C in IRON stations.  
150  
151  
152  
153  
154

## 155 **2.3 Airthings Corentium Plus**

156  
157 Airthings Corentium Plus (<https://airthings.com>) is a small sized commercial solid-state radon  
158 detector, providing also local storage for temperature, relative humidity and atmospheric pressure  
159 data. The instrument is battery supplied with autonomy of two years. Presently, we are testing five  
160 Corentium Plus in IRON stations.  
161  
162  
163  
164

## 165 **2.4 Durridge RAD7**

166  
167 Durridge RAD7 (<https://durridge.com/>) is a commercial electronic radon detector, generally  
168 employed for discrete measurements to assess the radon activity concentration in soil gas or  
169 dissolved in water. An electrostatic chamber, operated at a nominal voltage in the range 2,000 –  
170 2,500 V, is intended for radon daughters' collection onto the surface of a solid-state silicon detector,  
171 which detects and separates alpha particles on the basis of their energies. Only alpha decays from  
172 the short-lived <sup>218</sup>Po (its half-life is about 3 minutes) can be selected (Sniff mode, according to  
173  
174  
175  
176  
177  
178  
179  
180

181  
182  
183 RAD7 protocols) to rapidly infer  $^{222}\text{Rn}$ , since the radioactive equilibrium between them is reached  
184 in about 15 minutes. Temperature and relative humidity are recorded inside the instrument. A pump  
185 guarantees the circulation of the air in the set-up. INGV Radionuclide Laboratory operates two  
186 RAD7s used mainly for geochemical surveys.  
187  
188  
189  
190

## 191 **2.5 Barasol MC2 probe**

192 The Barasol MC2 is a commercial probe (<http://www.algade.com/>) used for measurements of radon  
193 in the ground (Papastefanou 2002). The unit is a cylindrical o-ring sealed device 62 mm in  
194 diameter, by approximately 520 mm long. It is constructed from fibreglass and corrosion-resistant  
195 stainless steel and weighs around 2 kg. Soil gas enters a detection volume through three cellulose  
196 filters that trap all the solid radon daughter products. The Barasol sensor is based on an implanted  
197 silicon detector with a depleted depth of 100  $\mu\text{m}$  and 400  $\text{mm}^2$  of sensitive area; counting is made  
198 by alpha spectrometry from decays of  $^{222}\text{Rn}$  and its daughter products created in the detection  
199 volume. MC2 sensitivity is typically 50  $\text{Bq m}^{-3}$  per pulse  $\text{h}^{-1}$ . It is designed to be used in  
200 environments where electricity and solar power supply are not available, guaranteeing one year of  
201 operating time with two type D alkaline batteries, and integrates the acquisition electronics and a  
202 local memory. The probe also records temperature and atmospheric pressure. INGV Radionuclide  
203 Laboratory and Osservatorio Etneo operate seven MC2 probes mainly for volcanic surveillance and  
204 specific research projects.  
205  
206  
207  
208  
209  
210  
211  
212  
213  
214

## 215 **2.6 AlphaNUCLEAR alphaMETER**

216 The commercial model 611 alphaMETER (<http://www.alphanuclear.com/index.html>) is intended  
217 for the detection, counting, and recording of alpha particle radiation from radon gas present in the  
218 near surface soil gas. The unit is a cylindrical o-ring sealed device 51 mm in diameter, 350 mm  
219 long. It is constructed from stainless steel and weighs 1.2 kg. One end is open to provide the  
220 sensitive volume for counting. At the top of this open-ended chamber, at approximately 65 mm in  
221 from that end is located the alpha particle sensitive detector. The detector is a silicon-diffused  
222 junction (DJ) with a sensitive surface area of 400  $\text{mm}^2$ . As this detector requires a dry, dark  
223 environment to operate, it is sealed behind a thin opaque film (6.35  $\mu\text{m}$  aluminized mylar) of  
224 sufficiently low density to efficiently pass alpha particles. This fragile sealing is protected by a  
225 plastic grill located approximately 12 mm from the open end of the sensitive volume. The internal  
226 electronics include a pulse amplifier/conditioner, the power regulator circuits, a real-time clock, a  
227 non-volatile data memory and a micro-processor devoted to perform all necessary house-keeping  
228  
229  
230  
231  
232  
233  
234  
235  
236  
237  
238  
239  
240

241  
242  
243 functions, as well as the pulse counting and RS-232 communications  
244 ([http://www.alphanuclear.com/manuals/611 Operating Manual V3.pdf](http://www.alphanuclear.com/manuals/611%20Operating%20Manual%20V3.pdf)). The sensitivity is around  
245 60 Bq m<sup>-3</sup> per pulse h<sup>-1</sup>. INGV Osservatorio Etneo has three alphaMETER used mainly for volcanic  
246 surveillance.  
247  
248  
249  
250

## 251 **2.7 Calibration facility**

252 In order to verify, calibrate and characterize the above listed instruments and, most important, to  
253 evaluate the absolute humidity impact on the detection efficiency of the silicon detector based  
254 instruments, ad-hoc experiments were designed (Figure 1).  
255  
256

257 We used a 56 L stainless steel radon chamber equipped with a scintillation cell (ZnS), not sensitive  
258 to humidity, coupled to a photomultiplier whose pulses are shaped by a signal processing module  
259 (D) and recorded by a multichannel analyzer (MCA) set in multiscaler mode (M). Counts C  
260 accumulated during the selected acquisition time, T<sub>acq</sub> (min), are stored in a channel (n), as a result a  
261 plot of C versus channels is available on the MCA screen. The radon activity concentration (A<sub>Rn CR</sub>)  
262 in the radon chamber at a generic time t = n\*T<sub>acq</sub> elapsed from the chamber switch on is given by  
263  
264  
265  
266  
267

$$268 A_{Rn CR}(t) = ((C(t) - B)/T_{acq}) / Cal_{CR} \quad (1)$$

269  
270  
271 where B is the background signal in the T<sub>acq</sub> time and Cal<sub>CR</sub> is the chamber calibration factor  
272 expressed as counts per minute (CPM) per Bq m<sup>-3</sup>.  
273  
274

275 Radon gas was extracted from an acidified (pH < 2) RaCl<sub>2</sub> source added with Ba (2,500 Bq), and  
276 injected in the chamber. Relative humidity and thus the amount of water molecules in the system, at  
277 given atmospheric pressure and temperature, were progressively varied by connecting the chamber  
278 to desiccant column (opening stopcocks O and Q and closing stopcocks P and R) or to a bubbling  
279 water bottle (opening stopcocks O and R and closing stopcocks P and Q) for drying or humidifying  
280 the closed circuit. When reached the desired conditions stopcock, P was opened and stopcocks O, Q  
281 and R were closed. The radon concentration within the chamber was always compared, for  
282 redundancy, with an online reference RAD7 (L) serviced and calibrated at least once per year at  
283 Durrige Company, Inc.  
284  
285  
286  
287  
288

289 Depending on the instrument to be calibrated, a mini chamber, a slave chamber or the generic  
290 instrument were connected to the chamber or inserted in the basic loop according to the following  
291 configurations:  
292  
293  
294  
295  
296  
297  
298  
299  
300

- Configuration A: an INGV instrument was connected to the B air tight connectors by means of a dedicated flange;
- Configuration B: the basic schematic, as is, with the generic RAD7 instrument instead of the reference one;
- Configuration C: a parallelepiped-shaped slave chamber made of steel containing small sized radon monitors was connected to the B air tight connectors. With a volume of around 28 L (430 mm x 180 mm x 360 mm) a maximum of 12 instruments can be power supplied and characterized at a time;
- Configuration D: a cylindrical mini chamber made of PVC equipped with proper flanges for AlphaNUCLEAR alphaMETER or Algade Barasol probes hosting was connected to the B air tight connectors. With a volume of 3.0 L ( $\Phi$  155 mm x 160 mm height) only one instrument can be characterized at a time.

Every instrument reading (counts or activity concentration) was compared with the activity concentration given at the same time by the radon chamber. A number of experiments were carried out according to a planned sequence of drying or humidification phases, if needed.

As a result, for A and D (AlphaNUCLEAR alphaMETER only) configurations, a calibration factor (Cal) was calculated as the ratio  $CPM_{INSTRUMENT} / A_{Rn CR}$  being  $CPM_{INSTRUMENT}$  the net counts per minute measured by the generic instrument and  $A_{Rn CR}$  the corresponding radon activity concentration ( $Bq/m^3$ ) in the radon chamber.

For B, C and D (Algade Barasol only) configurations, correction factors of activity concentration values obtained using RAD7, Algade AER, Airthings Corentium and Algade Barasol probes, defined as efficiency of the (electrostatic collection-based – only intended for RAD7) silicon detector, were calculated as the ratio  $A_{Rn INSTRUMENT}(t) / A_{Rn CR}(t)$  and plotted versus the amount of water in the instrument detection volume at the time t, being  $A_{Rn INSTRUMENT}$  the average radon activity concentration measured by the generic instrument and  $A_{Rn CR}$  the corresponding radon activity concentration in the radon chamber. It is important to point out that, in order to compare the behaviour of different instruments, and/or when the detection volume is a patented feature, AH (absolute humidity) shall be considered instead of the amount of water in the instrument detection volume.

In order to reduce uncertainties on the calculation of the above mentioned calibration or correction factors  $A_{Rn CR}(t)$  was calculated as in equation 1 by using the exponential interpolation  $C_1(t)$  of  $C(t)$  – B data available every  $T_{acq}$ , being  $C_1(t) = A * e^{B*t}$ , with the A and B parameters evaluated by OriginPro software (OriginLab™), where, in particular,  $-1/B$  is the interpolation time constant

(min) and  $t$  is the time (min) elapsed from the first acquired data to be considered.

It is worth noting that only radon chamber data recorded after at least 5 hours from radon enrichment or upon reaching the desired  $gH_2O$  (or AH) values were considered, to account for the establishment of new equilibrium conditions (secular equilibrium and/or radon diffusion within the new system configuration) and to reduce the error.

Water amounts in the detection volume, expressed as grams of water ( $gH_2O_{INSTRUMENT}$ ), are inferred from the psychrometric diagram as a function of the atmospheric pressure, temperature and relative humidity and calculated using equation 2, see details in De Simone et al., 2016 :

$$gH_2O_{INSTRUMENT} = AH * 1000 * \rho_{air\ T} * V_{INSTRUMENT} \quad (2)$$

where:

AH : absolute humidity (kg  $H_2O$  / kg dry air)

$\rho_{air\ T}$  : air density at a given temperature (kg/m<sup>3</sup>)

$V_{INSTRUMENT}$  : detection volume of the monitor (m<sup>3</sup>)

### 3. Results

#### 3.1 Configuration A

Configuration A (Figure 1) is adopted to calibrate and verify the linearity of INGV radon monitors. INGV radon monitors are operated with measurement cycles ranging from 15 to 120 minutes. On Arduino-based devices, counts are accumulated for an acquisition time that coincides with the time of the cycle. Old instruments with a proprietary data acquisition and storage board need a time during which the acquisition is idle: this is intended to modify the parameters stored (i.e. current date and time, calibration parameters), therefore a programmable timer is employed to schedule typically 120 minute cycles (minimum time due to a limitation on the admitted number of commutations) and set the acquisition time usually at 115 minutes, during the remaining 5 minutes the acquisition is idle. Net counts per minute, calculated subtracting the background signal of the scintillation cell provided by the manufacturer, are compared to the simultaneous mean concentration value in the radon chamber obtaining the calibration factor. As example, typical calibration factors, expressed as CPM / Bq m<sup>-3</sup>, for INGV radon monitors are reported in Table 1. Therefore, the activity concentration values  $A_{Rn\ INGV}$  are calculated according to the following

equation:

$$A_{Rn\text{ INGV}} (\text{Bq/m}^3) = (C/T_{acq} - B) / Cal \quad (3)$$

where:

$T_{acq}$  is the acquisition time (min)

C are the counts accumulated in  $T_{acq}$

B is the background signal of the scintillation cell (CPM), provided by the manufacturer. Also the accumulation of  $^{210}\text{Po}$  in the scintillation cell coating affects this value, and must be considered. Linearity has been verified since, after the secular equilibrium has been reached, counts decreases following an exponential trend  $C_0e^{-\lambda t}$  where  $\lambda$  is the radon decay constant.

### 3.2 Configuration B

Configuration B (Figure 1) is adopted to verify the built-in calibration of DurrIDGE RAD7 radon monitors, affected by absolute humidity. Water molecules are usually removed by a desiccant column placed upstream of the RAD7 instrument, however the assessment of RAD7 efficiency as a function of  $\text{gH}_2\text{O}$  is useful when the humidity cannot be reduced within a recommended range (0–0.002  $\text{gH}_2\text{O}$  inside the RAD7), for instance when water nearly saturates the desiccant column or under extreme climatic conditions (high temperatures).

Upon monitor connection AH ranging from less than 0.0007 to around 0.007  $\text{kg H}_2\text{O}$  per  $\text{kg}$  of dry air were obtained by properly operating stopcocks O, P, Q and R as stated above (see Figure 1). The average readings were compared with activity concentrations given by the radon chamber at each step. Correction factors of activity concentration values (defined as efficiency of the electrostatic collection-based silicon detector) to be applied when using RAD7 instruments were calculated as the ratio:

$$\text{Efficiency}(\text{gH}_2\text{O}) = A_{Rn\text{ RAD7 RAW}} / A_{Rn\text{ CR}} \quad (4)$$

and plotted versus  $\text{gH}_2\text{O}$ , being  $A_{Rn\text{ RAD7 RAW}}$  the average radon activity concentration measured by the RAD7 at water content  $\text{gH}_2\text{O}$  and  $A_{Rn\text{ CR}}$  the corresponding interpolated radon activity concentration in the radon chamber. The amount of water ( $\text{gH}_2\text{O}$ ) inside the RAD7 detection volume was inferred from the psychrometric diagram as a function of the atmospheric pressure, temperature and relative humidity according to Eq. 2. Typical efficiency trends are shown in Figure



2 along with the linear interpolation of data and the equation for the corrected activity concentration; please note that RAD7 S.N. 2226, which behaves better, had been recently serviced at Durrige laboratories (our experience confirms that RAD7 should be serviced, or just calibrated, at least once per year as recommended by Durrige Company and according to U.S. EPA 402-R-92-004 protocols when continuous radon monitors are concerned). Consequently, the RAD7 output ( $A_{Rn\ RAD7\ RAW}$ ) should be corrected according to the following equation we will refer to also for other instruments:

$$A_{Rn\ RAD7} = A_{Rn\ RAD7\ RAW} / \text{Efficiency}(gH_2O) \quad (5)$$

The relative efficiency of the silicon detector with respect to the scintillation cell decreases with the growth of the absolute humidity (AH), and thus with the water content expressed in  $gH_2O$  (g), inside RAD7. This dependence, with a fixed i) electrostatic chamber geometry and ii) nominal high voltage, is driven by the length of interaction of polonium atoms with water molecules, which impacts on the size of  $^{218}Po$  clusters and thus on the neutralization process. Temperature does not affect the efficiency of electrostatic collection-based silicon detectors (De Simone et al., 2016). Uncertainties induced by the above mentioned corrections, for  $0 < gH_2O < 0.006$ , are within those related to  $1\sigma$  of raw data concentrations values. For  $0.006 < gH_2O < 0.007$  uncertainties may be higher because of the detector response to the increased water content and neutralization process. In Figure 3 the linear behaviour is indirectly demonstrated plotting RAD7 concentrations, obtained at fixed low humidity values versus radon chamber concentrations.

### 3.3 Configuration C

Configuration C (Figure 1) is adopted to verify the built-in calibration of small sized radon monitors (Algade AER or Airthings Corentium). Since these devices were originally designed for indoor use, they are calibrated at typical indoor humidity values or, cautiously, at the maximum expected humidity. Again, the monitor responses can be corrected versus the absolute humidity expressed as  $kg_{H_2O}/kg_{dry\ air}$  and not as water in the detection volumes since they are very small in those instruments and, what's more, Airthings considers its value a patented feature. Algade AER and Airthings Corentium efficiency values versus AH are plotted in Figures 4 and 5, respectively, for two detectors. Equations obtained from linear interpolation in selected AH ranges are reported, representing the correction functions to be applied to the raw activity concentration data as in equation (5). At intermediate humidity values, the trend exhibits a similar change of slope as in De

541  
542  
543 Simone et al., 2016.  
544

545 The raw and corrected radon activity concentrations, AH and the reference radon activity  
546 concentration values are plotted in Figures 6 and 7 for Algade AER and Airthings Corentium,  
547 respectively. All the instrument responses adhere to the reference trend given by the radon chamber.  
548  
549 INGV operates an Algade customized version of the AER C instrument, not only aimed at  
550 radioprotection purposes, that comes from the factory with a pretty good built in calibration as a  
551 function of the AH. A cautious approach (raw concentration values always equal or greater than  
552 corrected concentration values) is not used and the raw concentration values are close to the ones  
553 from the radon chamber (and within a few per cent in dry conditions). A typical efficiency trend is  
554 shown in Figure 8; again, when corrections are applied to the raw data, AER C and radon chamber  
555 outputs are very similar (Figure 9).  
556  
557  
558  
559  
560

### 561 3.4 Configuration D

562 Configuration D (Figure 1) is adopted to calibrate the AlphaNUCLEAR alphaMETER Mod. 611 or  
563 verify the built-in calibration of Algade Barasol probes produced for outdoor soil gas monitoring.  
564 Again, correction trends as a function of the absolute humidity can be determined. As stated by  
565 AlphaNUCLEAR, the alphaMETER Mod. 611 is not sensitive to water molecules, the detector  
566 being protected by an opaque mylar sealing. Consequently, its calibration can be performed at  
567 standard environmental conditions. Sample calibration processes involving one or more instruments  
568 are outlined in Figures 10 and 11. Each probe linearity has been investigated by changing the radon  
569 concentration in the chamber from 5 to 38 kBq/m<sup>3</sup>. The calibration factors together with their  
570 uncertainties obtained i) at the highest activity concentration values available for each probe and ii)  
571 for the maximum number of observation for the best statistical conditions follow:  
572  
573  
574  
575  
576  
577  
578  
579

580  
581 **Cal<sub>AC-22</sub>** :  $0.000277 \pm 0.000023$  CPM/Bq m<sup>-3</sup>

582 **Cal<sub>AC-23</sub>** :  $0.000254 \pm 0.000024$  CPM/Bq m<sup>-3</sup>

583 **Cal<sub>AC-26</sub>** :  $0.000256 \pm 0.000025$  CPM/Bq m<sup>-3</sup>  
584  
585

586 For the linearity assessment all available data at different radon activity concentrations have been  
587 used:  
588  
589

#### 590 **AC-22 probe:**

591  $0.000268 \pm 0.000063$  CPM/Bq m<sup>-3</sup> , concentration in the range 4.8 – 5.2 kBq m<sup>-3</sup>

592  $0.000277 \pm 0.000023$  CPM/Bq m<sup>-3</sup> , concentration in the range 35 – 38 kBq m<sup>-3</sup>  
593  
594  
595  
596  
597  
598  
599  
600

601  
602  
603 **AC-23 probe:**

604  $0.000253 \pm 0.000056$  CPM/Bq m<sup>-3</sup>, concentration in the range 5.3 - 6 kBq m<sup>-3</sup>

605  $0.000254 \pm 0.000024$  CPM/Bq m<sup>-3</sup>, concentration in the range 32 - 34 kBq m<sup>-3</sup>

607  
608 **AC-26 probe:**

609  $0.000258 \pm 0.000052$  CPM/Bq m<sup>-3</sup>, concentration in the range 4.6 – 5.2 kBq m<sup>-3</sup>

610  $0.000256 \pm 0.000025$  CPM/Bq m<sup>-3</sup>, concentration in the range 26 - 30 kBq m<sup>-3</sup>

611  
612  
613 Therefore, the linear behaviour of the instruments has been verified, within the statistical error  
614 which is greater at low concentration values.  
615

616  
617 **3.5 Electrical shielding**

619 For those devices mostly used in outdoor permanent monitoring stations (i.e. INGV and Alcade  
620 AER instruments), we have also investigated the possibility of external perturbations associated  
621 with atmospheric electromagnetic phenomena (i.e. lightnings). As it is known, the lightning is a  
622 current discharge of 2-200 kA on a voltage of 1-10 GV for duration of up to 1.5 s, which generates  
623 a broad-spectrum electromagnetic (EM) emission of several MHz of extension. Most of the EM  
624 radiation is limited to the low frequencies, which can penetrate the masonry and reach the  
625 basements.  
626  
627

628  
629 To test this hypothesis, a piezoelectric generator was used to produce an electrical spark of at least  
630 1000 V and about 2 mm in length. This can be considered a wide-spectrum EM source that, from  
631 the analysis of the EM signal in the ELF-VLF spectrum, seems to fairly simulate the lightning  
632 emission.  
633

634  
635  
636 Actually only INGV instruments proved to be vulnerable to close exposure (less than 6 cm) of the  
637 small electric spark and as a matter of fact they produced spurious counts. Each compression cycle  
638 of the piezoelectric crystal caused about 10 spurious counts. We observed also that un-shielded  
639 INGV sensors were sensitive to electromagnetic field of mobile phone, placed very close to the  
640 instrument.  
641  
642

643  
644 After this test, we investigated the electrical shielding of different versions of INGV proprietary  
645 instruments. The  $\mu$ -metal tube intended for electromagnetic protection is not grounded. Besides, we  
646 observed that the sensitive element was the pulse shaping electronics together with its unshielded  
647 input cable, placed in front of the photomultiplier. The electrical shielding of these two elements  
648 definitively solved the problem of spurious counts generation.  
649

650  
651 Shielded INGV sensors will now be tested on site, together with original sensors, to experimentally  
652 test the hypothesis of thunderstorm interference, checking also available online lightning maps for  
653  
654  
655

661  
662  
663 real time presence and frequency of events near radon monitoring stations (i.e.,  
664 [www.lightningmaps.org](http://www.lightningmaps.org)).  
665  
666  
667  
668

#### 669 **4 Conclusions**

670 A radon chamber available at the INGV Radionuclide laboratory has been used to verify, calibrate  
671 or even characterize instruments for the measure of soil gas or indoor radon activity concentration.  
672 The influence of water content in the detection volume has been accounted for, affecting solid-state  
673 detectors installed in various instruments. The instruments have also been tested and implemented  
674 for electrical shielding.  
675  
676  
677  
678

679 The response of every radon monitor installed in the IRON network has been verified and  
680 calibrated, also as a function of the absolute humidity depending on the kind of instrument, yielding  
681 comparable results as shown in Figure 12. Consequently, all the recorded trends are suitable, as is,  
682 for further analysis techniques.  
683  
684

685 Remarkably, low cost radon detectors originally designed for indoor use, after applying our  
686 procedures, exhibit performances (within their sensitivity figures) comparable with those granted by  
687 devices specifically designed for scientific applications and can be operated reliably in high  
688 performance monitoring networks like IRON.  
689  
690  
691  
692  
693  
694

#### 695 **References**

696  
697  
698 Cannelli, V., 2017. IRON-DB: a database for the Italian Radon mOnitoring Network, Rapporti  
699 Tecnici INGV, n.371 2017, <http://www.ingv.it/editoria/rapporti/2017/rapporto371/>  
700  
701

702 Cannelli, V., Piersanti, A., Galli, G., Melini, D. Italian Radon mOnitoring Network (IRON): A  
703 permanent network for near real-time monitoring of soil radon emission in Italy, 2018. *Annals of*  
704 *Geophysics*, 61(4), doi:<http://dx.doi.org/10.4401/ag-7604>.  
705  
706

707 Chu, K-D., and Hopke, P.K., 1988. Neutralization Kinetics for Polonium-218. *Envir. Sci. Tech.* 22,  
708 711-717.  
709  
710

711 De Simone G., Lucchetti C., Galli G., Tuccimei P., 2016. Correcting for H<sub>2</sub>O interference using  
712 electrostatic collection-based silicon detectors. *Journal of Environmental Radioactivity*. Volumes  
713 162-163, 146-153. <https://doi.org/10.1016/j.jenvrad.2016.05.021>.  
714  
715  
716

721  
722  
723 Hopke, P.K., 1989. Use of electrostatic collection of  $^{218}\text{Po}$  for measuring Rn. *Health Phys.* 57, 39-  
724 42.

725  
726  
727 Papastefanou, C., 2002. An overview of instrumentation for measuring radon in soil gas and  
728 groundwaters, *Journal of Environmental Radioactivity*, Volume 63, Issue 3 (2002), Pages 271-283,  
729 ISSN 0265-931X, [http://dx.doi.org/10.1016/S0265-931X\(02\)00034-6](http://dx.doi.org/10.1016/S0265-931X(02)00034-6)  
730

731  
732 Roca, V., De Felice, P., Esposito, A.M., Pugliese, M., Sabbarese, C., Vaupotich, J., 2004. The  
733 influence of environmental parameters in electrostatic cell radon monitor response. *Appl. Radiat.*  
734 *Isot.* 61, 243–247.  
735

736  
737 Tuccimei, P., Moroni, M., Norcia, D., 2006. Simultaneous determination of  $^{222}\text{Rn}$  and  $^{220}\text{Rn}$   
738 exhalation rates from building materials used in Central Italy with accumulation chambers and a  
739 continuous solid state alpha detector: Influence of particle size, humidity and precursors  
740 concentration. *Appl. Radiat. Isot.* 64, 254–263.  
741

742  
743  
744 U.S. Environmental Protection Agency. Office of Air and Radiation (6604J). 1992. Indoor Radon  
745 and Radon Decay Product Measurement Device Protocols. EPA 402-R-92-004  
746  
747

## 748 749 750 751 752 **Figure captions**

753  
754  
755 **Fig. 1** Experimental set-up. A) radon chamber; B) air tight connectors (CPC) to be used when air  
756 circulation needs a pump; C) air tight connectors (CPC) when air circulation is guaranteed by an  
757 outer device; D) signal processing module; E) photomultiplier; F) scintillating flask; G) fan; H)  
758 desiccant column; I) humidifying device; L) DurrIDGE RAD7 (required for Configuration B); M)  
759 multiscaler, N) low voltage supply; O), P), Q) and R) stopcocks. Configuration A: INGV radon  
760 sensor connected to the radon chamber. Configuration B (basic experimental set-up): DurrIDGE  
761 RAD7 connected to the radon chamber. Configuration C: small sized instruments (i.e. Algade AER,  
762 Airthings Corentium) contained in a medium sized external box connected to the radon chamber.  
763 Configuration D: soil gas probes coupled to a small sized external box connected to the radon  
764 chamber.  
765  
766  
767  
768  
769  
770

771  
772  
773 **Fig. 2** Efficiency trends versus the water content exhibited by two RAD7s. Equations for corrected  
774 activity concentration values are reported.  
775

781  
782  
783  
784  
785  
786  
787  
788  
789  
790  
791  
792  
793  
794  
795  
796  
797  
798  
799  
800  
801  
802  
803  
804  
805  
806  
807  
808  
809  
810  
811  
812  
813  
814  
815  
816  
817  
818  
819  
820  
821  
822  
823  
824  
825  
826  
827  
828  
829  
830  
831  
832  
833  
834  
835  
836  
837  
838  
839  
840

**Fig. 3** Verification of the linear behaviour of a RAD7 instrument.

**Fig. 4** Sample Algade AER efficiency versus AH. Equations for corrected activity concentration values are reported.

**Fig. 5** Sample Airthings Corentium efficiency versus AH. Equations for corrected activity concentration values are reported.

**Fig. 6** Correction of the built-in calibration factor for an Algade AER.

**Fig. 7** Correction of the built-in calibration factor for an Airthings Corentium.

**Fig. 8** Algade AER efficiency versus AH of a customized instrument. Equation for corrected activity concentration values is reported.

**Fig. 9** Correction of the built-in calibration factor for a customized Algade AER.

**Fig. 10** Background assessment, calibration and linearity check of one AlphaMETER probe.

**Fig. 11** Operating sequence of a radon chamber to calibrate AlphaNUCLEAR alphaMETER probes. At least two radon concentrations have been used to check each probe linearity, except for the damaged AC-40.

**Fig. 12** Comparison of INGV, AER and Corentium radon monitors connected to a radon chamber.

841  
842  
843  
844  
845  
846  
847  
848  
849  
850  
851  
852  
853  
854  
855  
856  
857  
858  
859  
860  
861  
862  
863  
864  
865  
866  
867  
868  
869  
870  
871  
872  
873  
874  
875  
876  
877  
878  
879  
880  
881  
882  
883  
884  
885  
886  
887  
888  
889  
890  
891  
892  
893  
894  
895  
896  
897  
898  
899  
900

## Tables

**Table 1** Typical calibration factors of INGV radon monitors

Sensor Id.	Cal (CPM / Bq m <sup>-3</sup> )
RNM_INGV_03_01	0.0513 ± 0.0005
RNM_INGV_03_02	0.0715 ± 0.0008
RNM_INGV_03_03	0.0689 ± 0.0007
RNM_INGV_03_04	0.0706 ± 0.0012
RNM_INGV_03_05	0.0650 ± 0.0009
RNM_INGV_03_06	0.0692 ± 0.0012
RNM_INGV_03_07	0.0653 ± 0.0009

Figure 1

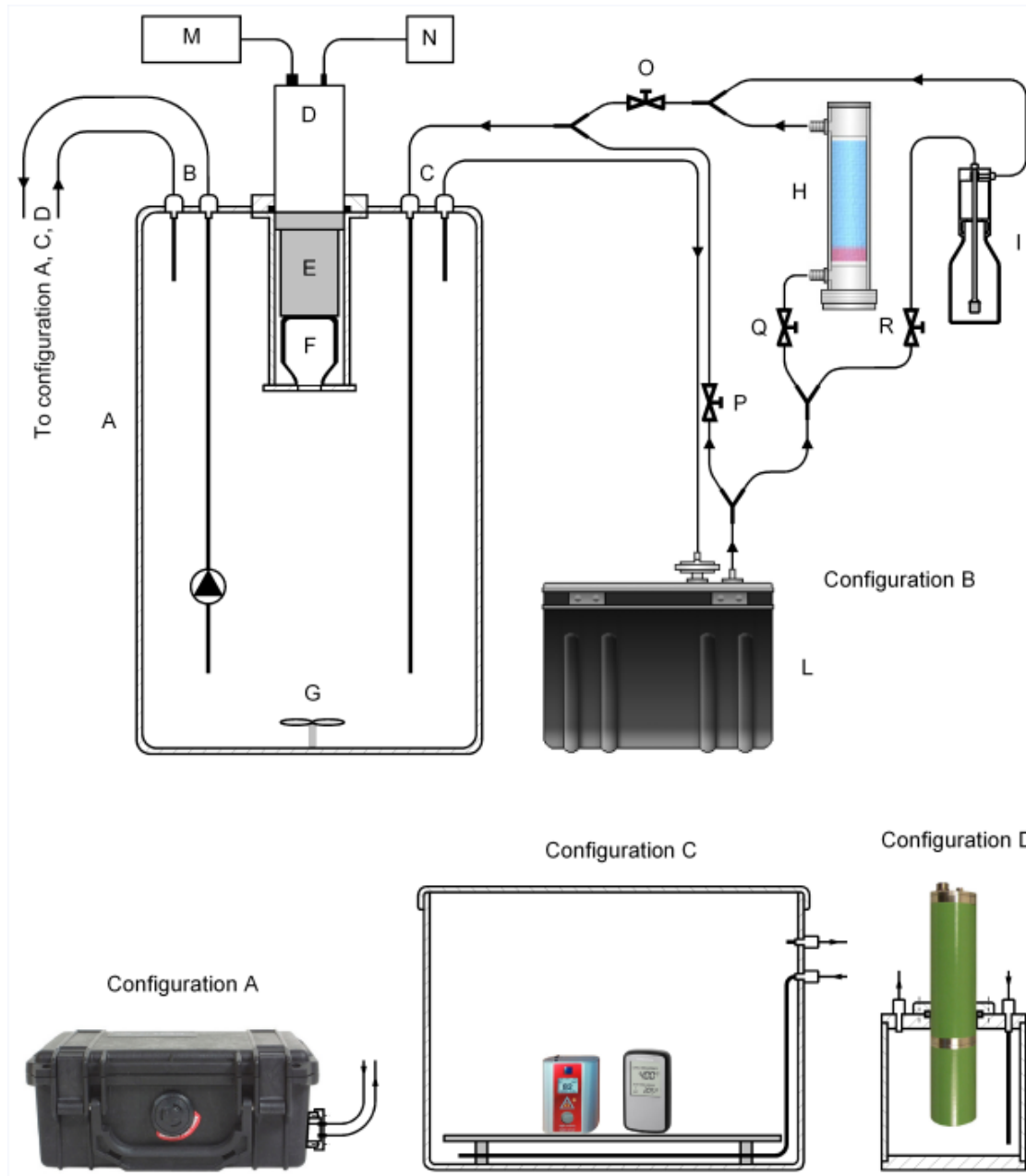




Figure 2

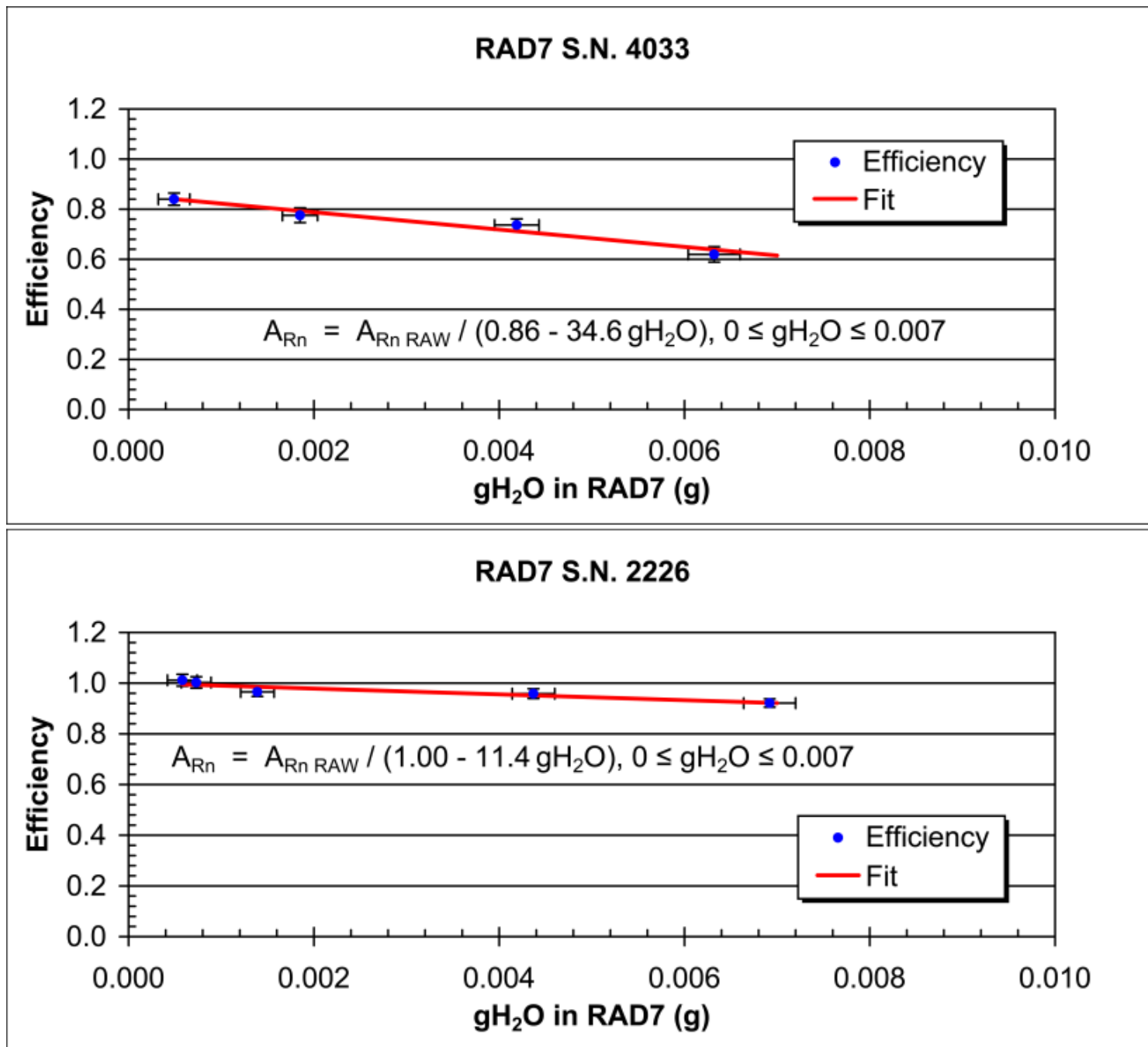


Figure 3

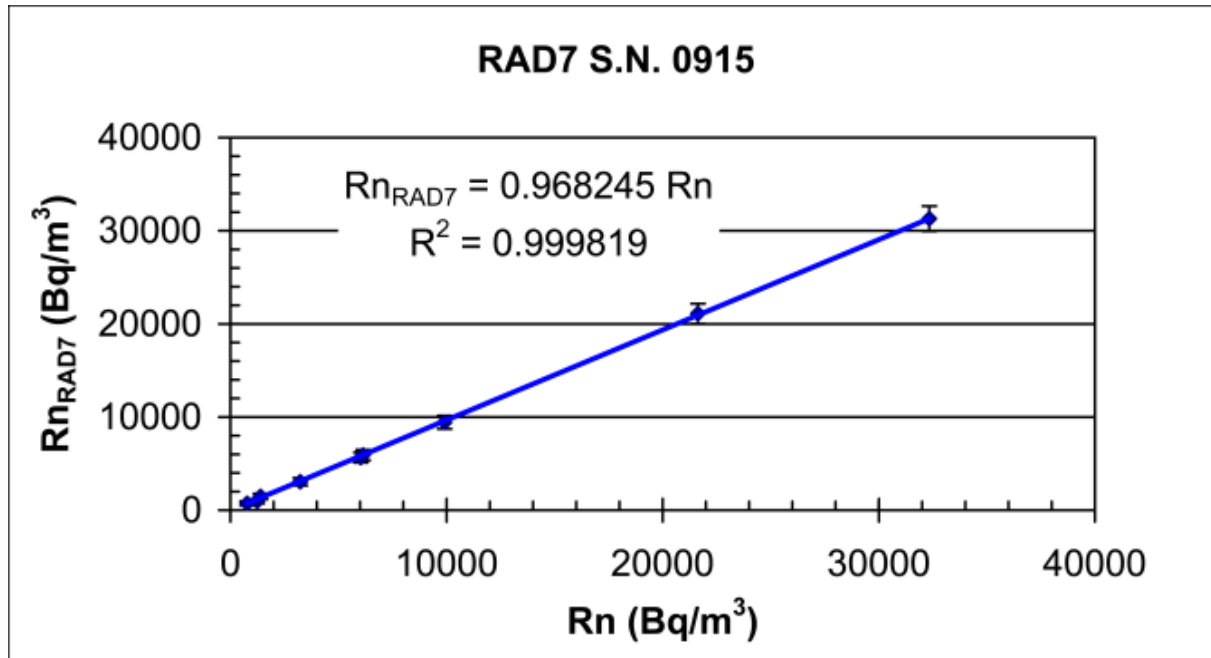


Figure 4

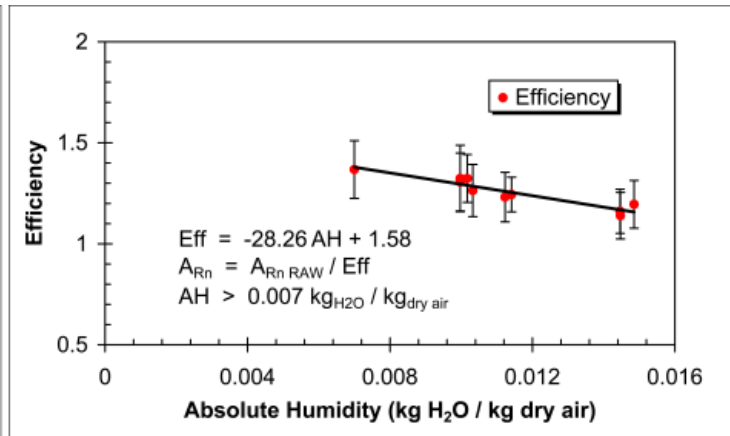
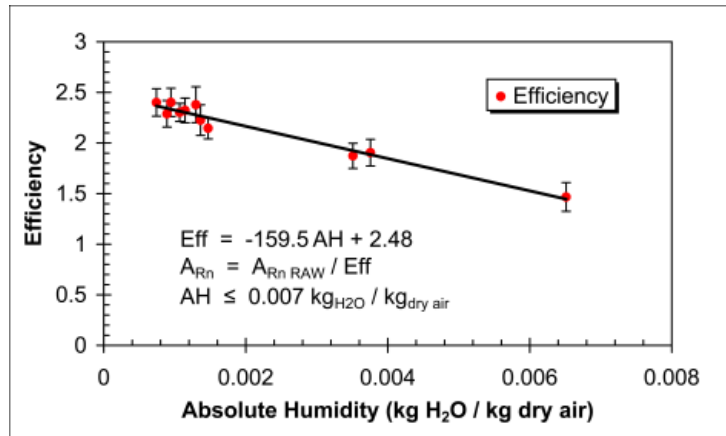


Figure 5

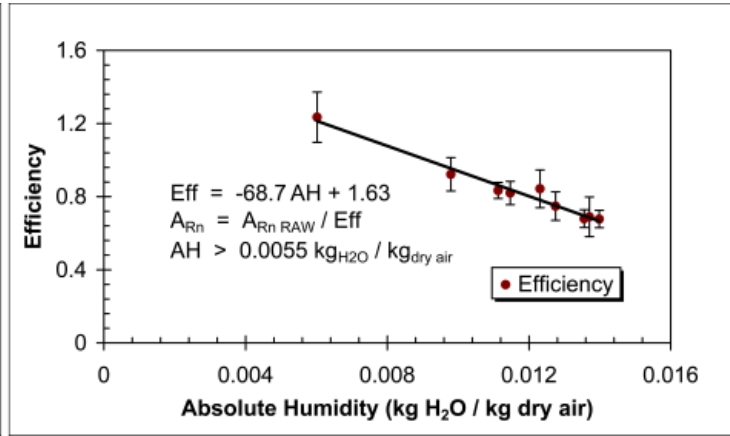
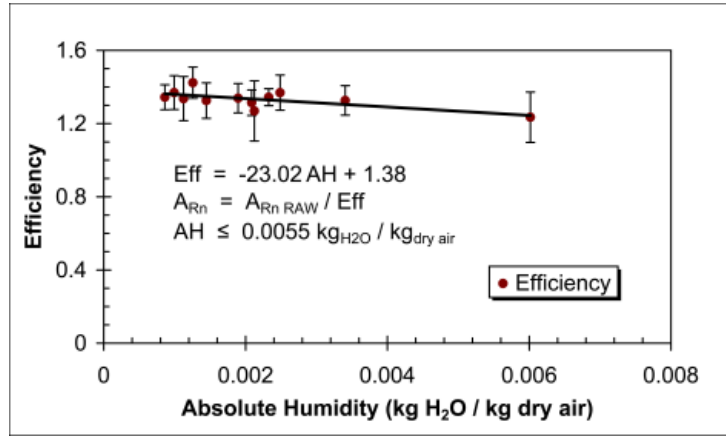


Figure 6

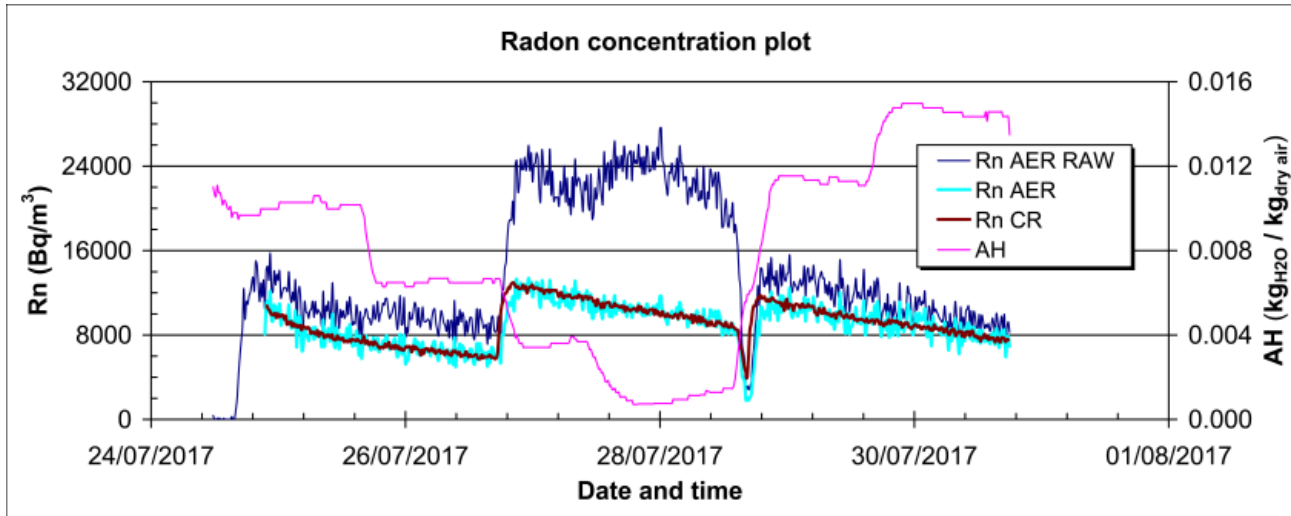


Figure 7

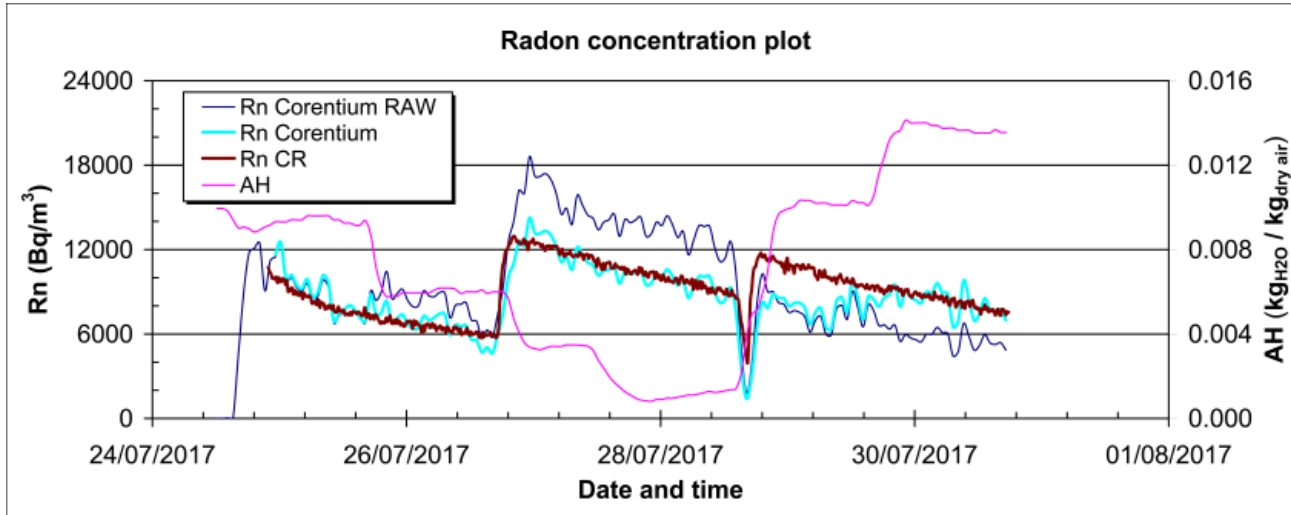


Figure 8

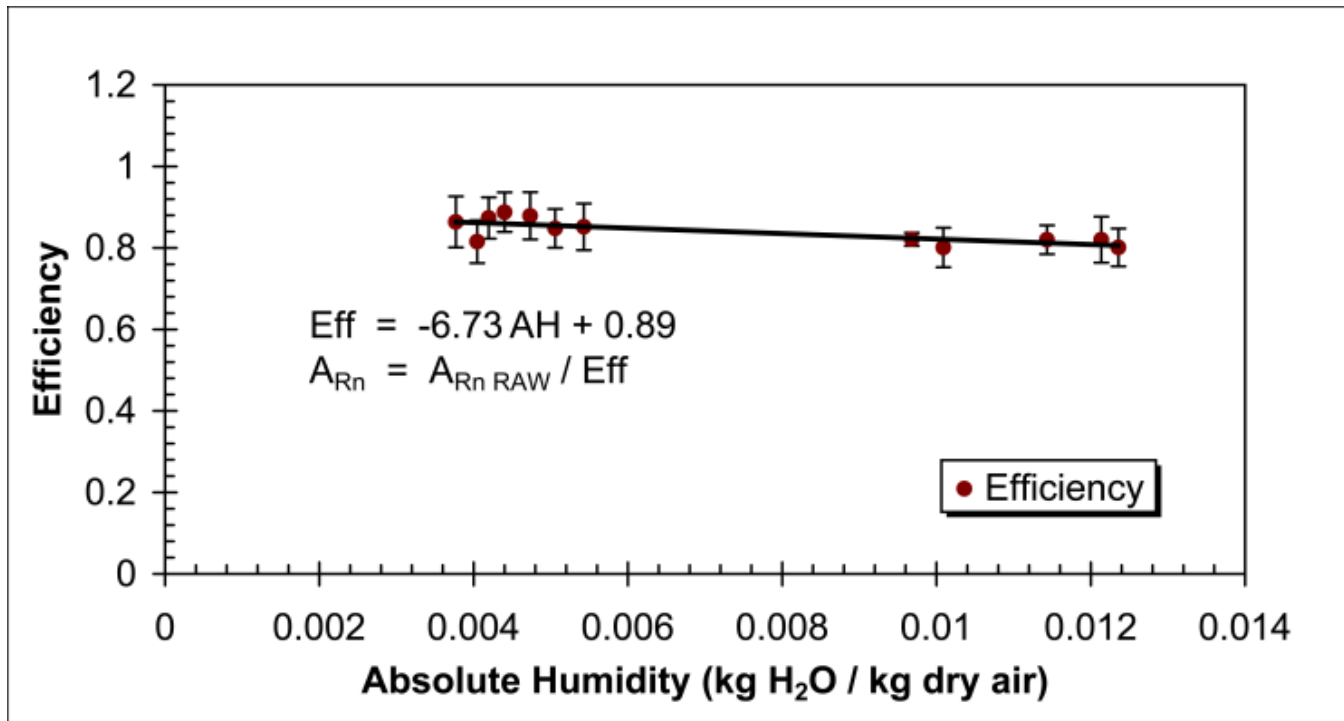


Figure 9

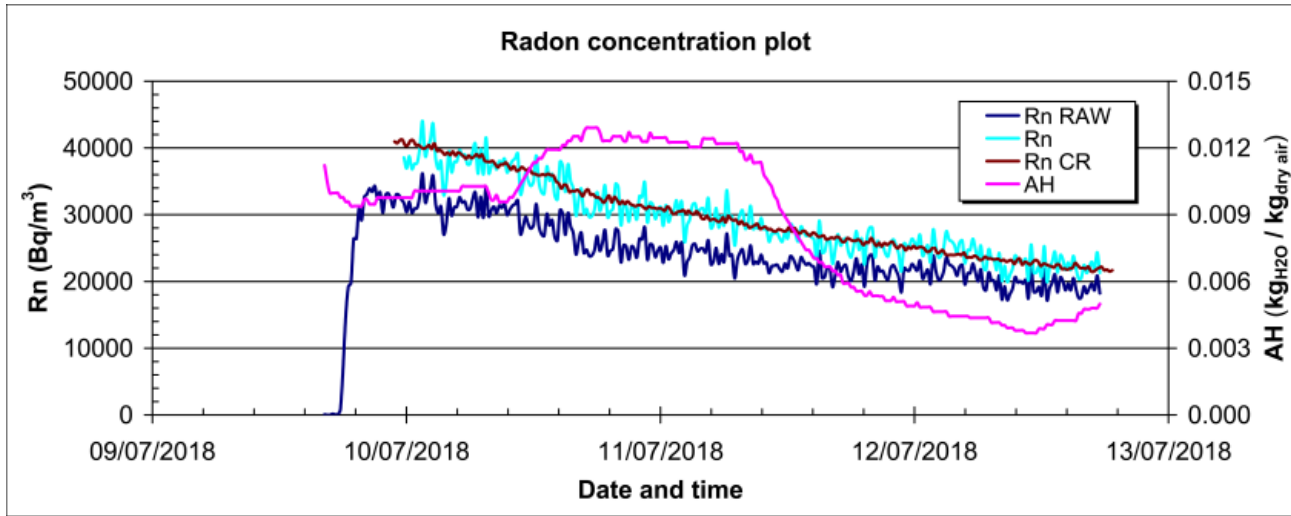




Figure 10

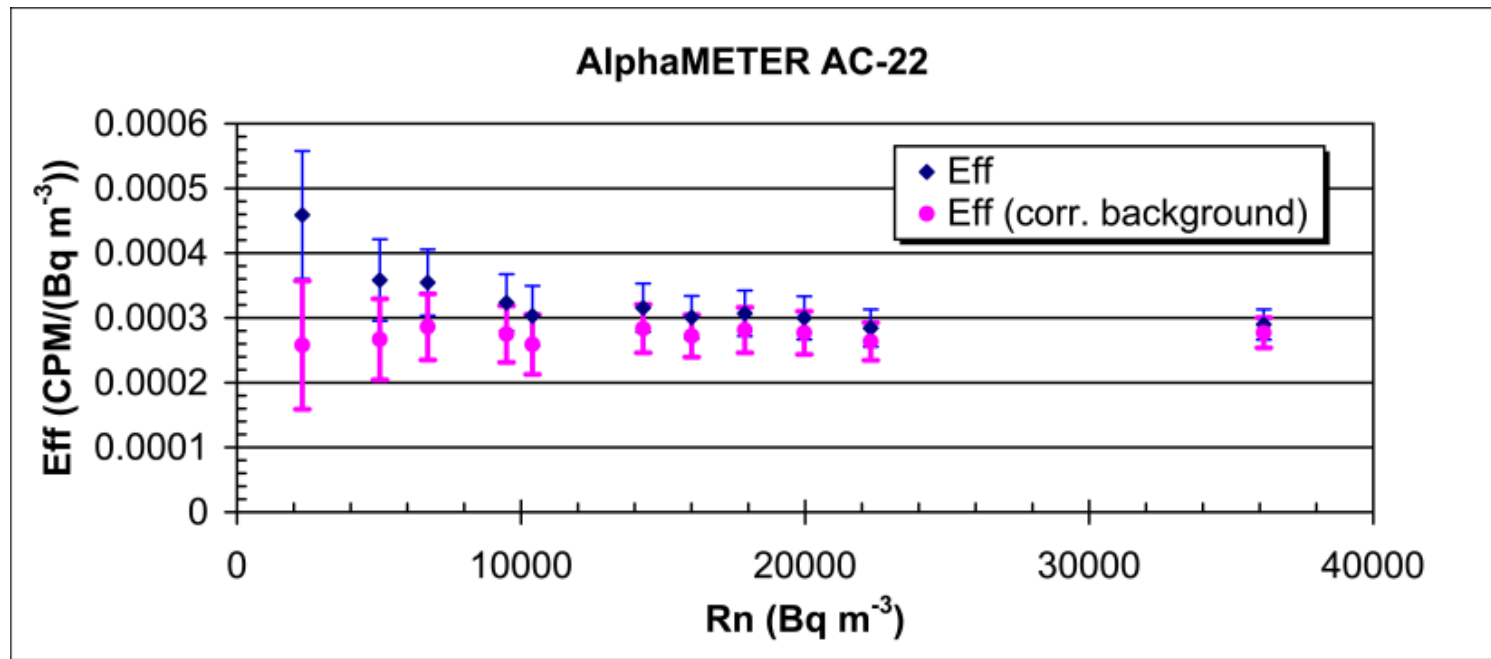


Figure 11

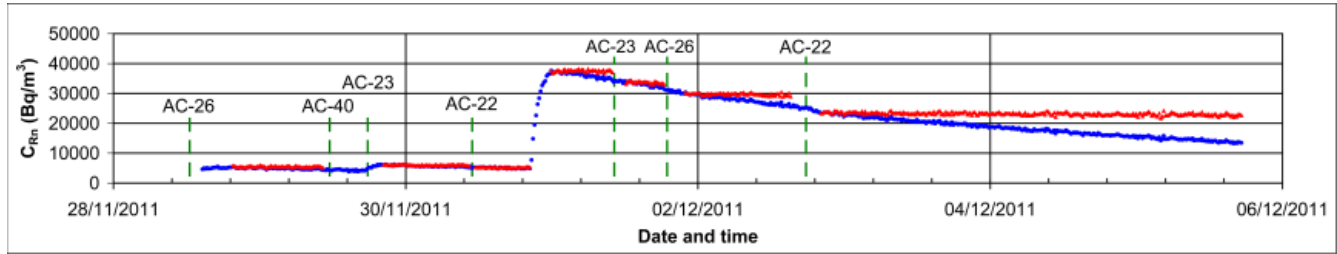


Figure 12

